

Received 19 June 2022, accepted 17 July 2022, date of publication 24 August 2022, date of current version 19 September 2022.

Digital Object Identifier 10.1109/ACCESS.2022.3201235



Automatic Meter Reading Based on Bi-Fusion MSP Network and Carry-Out Rechecking

JIA-YUAN LIAO¹, JUN-WEI HSIEH^{ID2}, (Member, IEEE), AND CHING-WEN MA²

¹Department of Computer Science Engineering, National Taiwan Ocean University, Keelung 202301, Taiwan

²College of Artificial Intelligence, National Yang Ming Chiao Tung University, Tainan 71150, Taiwan

Corresponding author: Jun-Wei Hsieh (jwhsieh@nycu.edu.tw)

ABSTRACT Automatic meter reading is important for power billing in a smart city. Most SoTA (State-of-the-Art) vision-based methods can read only cyclometers and fail to handle dial meters due to their in-between problem and ambiguous patterns to interpret a digit and are not light enough to be run on an embedded platform. This paper focuses on the design and development of an Internet of Things (IoT)-assisted real-time Automatic Meter Reading (AMR) system for utility billing in a smart city. To enhance the accuracy of object detection, most SoTA methods use a very deep CNN-based architecture to create rich feature maps. However, this backbone also makes small objects in the last layer become one pixel or less. This paper proposes a novel BI-Fusion Mixed Stage Partial (BIF-MSP) network to hold the spatial information of a smaller object at the end of network architecture and also increase the efficiency while operating on an embedded system. It can accurately detect small digits not only from cyclometers but also from dial meters. It can automatically decide a rule (anticlockwise or clockwise) to accurately read digits on a dial-type meter. After that, a carry-out re-checking module is proposed to further improve the accuracy of this AMR system. The experiments show the superiorities of our ARM system in terms of accuracy and efficiency. The dataset can be publicly accessed from the following URL: <http://140.113.110.150:5000/sharing/52HCvjly2>

INDEX TERMS Automatic meter reading, bi-fusion, deep learning, power billing, object detection, YOLO.

I. INTRODUCTION

Automatic Meter Reading (AMR) [1], [2] is the remote collection of consumption, diagnostic, and status data from water meters or energy meters (gas, electric) and transferring those data to a central database for billing, troubleshooting, and analysis. This AMR system is important for utility billing in a smart city [3] and can save utility providers the expense of periodic trips to each physical location to read meter data. Although smart meters have been used in some countries, there are still many traditional meters working together for utility billing. For example, as reported in [4] and [5], there are still many nonautomatic meters to be found in the United States, and they are difficult to replace due to expensive costs and building regulations. Thus, reading electric meters in these countries is still performed manually with errors. Such errors can be avoided if smart meter reading



FIGURE 1. Two types of electricity meters. (a) Dial meter. (b) Cyclometer.

sensors are adopted to check the devices. Then, the meter data can be securely sent to the service provider through a privacy-preserving access protocol [6], [7] in an IoT-enabled smart-grid system to do billings in near real time without involving man efforts.

Many vision-based reading systems [5], [6], [7], [8], [9], [10], [11], [12], [13], [14], [15], [16], [17], [18], [19] have been proposed for utility meter recognition

The associate editor coordinating the review of this manuscript and approving it for publication was Chiu-W. Sham^{ID}.

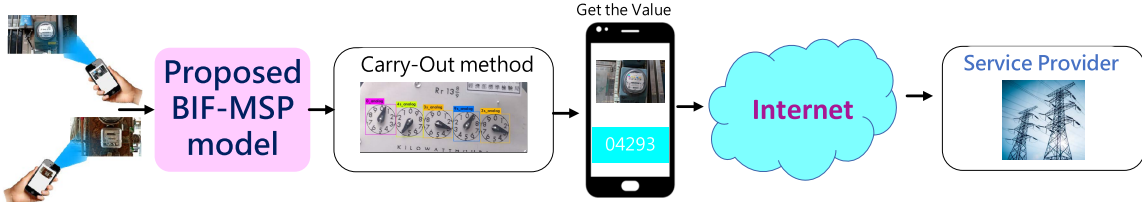


FIGURE 2. Diagram of our AMR system for meter digit reading.

based on handcrafted or deep features. For example, Rodriguez *et al.* [8] used a color-slicing method to isolate digital numbers and then recognized them based on their Hausdorff distances. In [10], Gallo, Zamberletti, and Noce proposed a segmentation-based method to extract characters for the reading of meters based on the technique of Maximally Stable Extremal Regions (MSER) [11], but failed with blurred images caused by perspective distortions. In [9], Tang *et al.* used a binarization method to threshold an energy meter and then adopted morphological operations to remove noise so that its embedded digits were recognized. In recent years, deep Convolutional Neural Networks (CNN) have been widely used in different computer vision tasks with superior performance in object detection [20], [21], [22]. The features extracted by CNNs are often more general, accurate, and less affected by different environmental conditions. For example, in [12], Li *et al.* used a new lightweight CNN to recognize the digits of the cyclometer meters. G’omez, Rusiñol, and Karatzas [13] used a CNN-based method to detect and recognize digits on utility meters. As shown in FIGURE 1, there are two types of meters, the cyclometer meter and dial-type one. Compared with a cyclometer, two challenges force a dial meter to be more difficult to recognize. The first challenge is caused by the ambiguity of the interpretation rule for reading a dial. A dial can be interpreted by an anticlockwise rule or a clockwise rule according to its positions. The second challenge is the “in-between” problem of a dial caused by its analog nature; that is, the status of a dial is continuous rather than discrete. Thus, a dial will not exactly point to a digit, but often to an “in-between” position between two adjacent digits. The “in-between” position often confuses the above hand-crafted or deep approaches and therefore results in reading errors on the digits. It is noticed that the “in-between” problem is also seen when recognizing a cyclometer.

This paper focuses on the design and development of an Internet-of-Things (IoT) assisted real-time automatic meter reading (AMR) system for utility billing in a smart city. It should be a light architecture and can read both cyclometers and dial meters. To enhance object detection accuracy, most SoTA methods use a much deeper CNN architecture to create rich feature maps. As claimed in [40], [41], deepening the CNNs not only can solve the vanishing gradient but also makes small objects in the last layer be one pixel. The one-pixel feature makes classification and bounding box regression very hard. Thus, most SoTA CNN-based object detectors, e.g., RefineDet [34] or Faster R-CNN [20], are

problematic for small object detection. In addition, the deeper structure will lose its efficiency due to the design of a much deeper network architecture and will become unsuitable for edge computing devices. In real-life testing, the efficiencies of the above SoTA CNN detectors on embedded systems such as TX2 are shown to be less than 3 fps for frame dimension 416×416 . To address the above challenges, a novel AMR system is proposed in this paper. FIGURE 2 shows its diagram. First, a novel BI-Fusion Mixed Stage Partial (BIF-MSP) network is proposed to detect and recognize both cyclometers and dial meters. This BIF-MSP network can hold the spatial information of a smaller object at the end of the network and also increase efficiency while operating on an embedded system. Then, to deal with the ambiguity of reading rule in recognizing a dial-type meter, this paper proposes a label-sharing technique to make two clockwise and anticlockwise dials share the same label and then identify their real values according to their positions. To address the “in-between” problem, a new rechecking method is proposed to determine the actual values of the digits on a meter according to their carry-out conditions. Our proposed AMR system adopts the above two methods to accurately detect and recognize both small digits and dials even with significant distortions. Its efficiency on TX2 is up to 30 fps. The main contributions of this paper are summarized as follows:

- 1) A novel AMR system is proposed to read information from both cyclometers and dial meters in real time.
- 2) Furthermore, a BIF-MSP network is proposed to detect small digits or dials even with significant distortions and can achieve 30 fps on TX2.
- 3) A carry-out rechecking method is proposed to further improve the accuracy of meter reading.
- 4) The AMR system can automatically decide on a correct reading rule (anticlockwise or clockwise) to read each dial on a dial meter.
- 5) The AMR system can be run directly on an embedded device to analyze the acquired image so that only the recognized data needs to be transferred.
- 6) Extensive experiments show the superiority of our AMR system in reading both cyclometers and dial meters in terms of accuracy and efficiency.

II. RELATED WORKS

In the literature, different frameworks [14], [15], [16], [17], [18] have been proposed for AMR based on hand-crafted features. For example, Shu, Ma, and Jing [14] proposed a segmentation-based method to extract text candidates and

then recognize their digits by OCR. In [15], Oliveira, Santos, and Bensebaa used a homomorphic filter to reduce the effect of illumination and then adopted a K-mean clustering scheme to recognize all digits on Watt hour meters. Rodriguez *et al.* [8] assumed that all digits were not occluded and then detected and recognized the digits from an electrical meter based on their Hausdorff distances. In [16], Cai, Wei, and Yuan used a projection technique to segment digits from a meter and then recognized them based on Back-Propagation (BP) networks. Similarly to [16], Zhang *et al.* [17] used a thresholding method to segment text regions from a household meter and then recognized all embedded digits by BP networks. In [10], a multilayer perceptron was trained to extract text regions and then an MSER method was adopted to extract and recognize individual digits according to their histogram of oriented gradient features. Furthermore, after intensity normalization, Elrefaei *et al.* [18] took advantage of gray and location distributions to detect and read the digits on a meter through a smartphone. In [19], Anis *et al.* used morphological operations to extract text regions from an electric meter and then adopted horizontal and vertical projections to segment and recognize all individual digits. However, compared to deep features, the above handcrafted features perform worse and more unstable to read information from meters, especially under poor lighting conditions.

Recently, the accuracy of object detection has been improved by a large margin with various SoTA models such as FPN [20], YOLOv3 [22], and SSD [21]. With these advances, many frameworks for CNN-based AMR have been proposed. For example, in [13], Gomez, Rusinol, and Karatzas proposed a segmentation-free system to detect digits in a meter based on CNNs. Laroca *et al.* [23] designed a two-stage framework for counter detection and recognition based on a YOLO detector. In [28], Son *et al.* also used a YOLO detector to read the digits on a gas meter. Instead of using YOLO, Tsai *et al.* [29] trained an SSD (Single Shot MultiBox) [21]-based detector to detect digits from a digit meter. YOLO-based and SSD-based detectors are efficient, but perform poorly for small object detection. In [30], Waqar *et al.* proposed a scale-invariant approach based on Faster R-CNN [20] to detect small digits on a meter under different lighting conditions. Furthermore, Gao *et al.* [31] used CNNs for feature extraction and then adopted a Bidirectional Long Short-Term Memory (BLSTM) scheme for end-to-end sequence alignment to recognize the digits of water meters based on mobile devices. Instead of BLSTM, Yang *et al.* [32] used a Recurrent Neural Network (RNN) for sequence modeling and then recognized the digits of water meters. For mobile applications, Li *et al.* [33] proposed a PGC (Pressure Gauge Calibration) sequence network with three convolutional layers to recognize the digits of pressure gauge meters for fast and accurate gauge calibration. For performance evaluation, Laroca *et al.* [23] introduced a public dataset, called the UFPR-AMR dataset, to evaluate different CNN-based approaches for AMR. CNN-based approaches above can recognize digits only for digit-type

meters, but cannot analyze dial-type meters due to their “in-between” positions. This paper proposes a new AMR system to read data not only from cyclometers but also from dial meters under different lighting conditions. It can automatically decide on a correct rule (anticlockwise or clockwise) to interpret dials in a dial-type meter, even on embedded devices.

III. METHOD

Most current AMR systems are character-based and only recognize digits (0-9). However, there are still various dial-type meters used in household measuring devices. To reduce human effort and manpower, it is better to design a light CNN architecture to read both cyclometers and dial meters on an embedded system. As shown in FIGURE 2, a light BIF-MSP architecture is proposed to detect counter regions from which different digits are extracted. With the help of this BIF-MSP architecture and carry-out rechecking, our proposed AMR system can effectively deal with the “in-between” problem and the interpretation-ambiguity problem, i.e., digits interpreted by an anticlockwise rule or a clockwise rule. More importantly, the proposed AMR system can run on an embedded system to directly recognize a meter instead of on a server. In what follows, details of the BIF-MSP architecture are first introduced, and then the details of our AMR system are discussed.

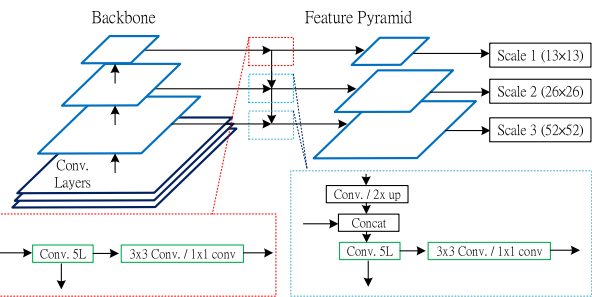


FIGURE 3. Feature pyramid in YOLO3.

A. CONCATENATED FEATURE PYRAMID NETWORK

To improve the accuracy of small object detection, a feature pyramid (FP) structure is commonly adopted in the SoTA detectors due to its multiscale structure. For example, the YOLOv3 architecture is created by adding an FPN layer in the YOLOv2 network and replacing the swallower backbone (DarkNet19) with a deeper backbone (DarkNet53) for small object detection. FIGURE 3 shows the detailed diagram of the YOLOv3 architecture. However, as claimed in [40] and [41], deepening the CNNs can not only solve the vanishing gradient, but also make small objects in the last layer become one pixel due to subsampling layers. The one-pixel feature makes classification and bounding box regression very hard. To improve the ability of small object detections due to the small size of the top feature maps, which are less than 1 pixel, this paper proposed a BIF-MSP architecture to increase the accuracy of small object detection. It first creates a Concatenated Feature Pyramid (CFP) and a Bi-Fusion module for

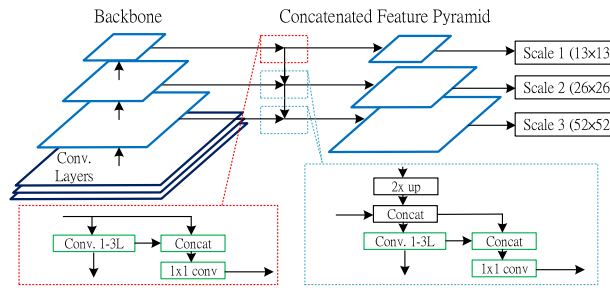


FIGURE 4. Proposed concatenated feature pyramid (CFP).

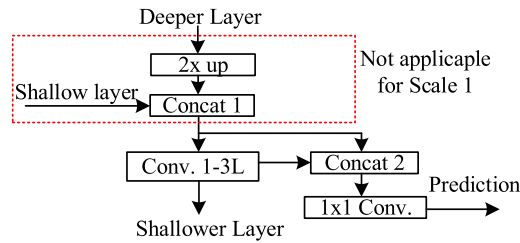


FIGURE 5. Proposed Concatenation Block (CB), consisting of two concatenations, 2 \times upscaling operation, and 2-4 convolutional layers. (Conv. 1-3L) refers to 1-3 convolutional layers.

fusing feature maps with top-down and bottom-up mechanisms to generate flexible FPs for small object detection.

This CFP is shown in FIGURE 4 and has some similarities to FPN and YOLOv3, whereby we use feature pyramids to detect objects on three different scales. The objective of CFP is to increase and adjust the accuracy and efficiency of small object detection in embedded devices. To achieve this, the CFP includes an inter-scale Concatenation Block (CB), shown in FIGURE 5, consisting of a reduced number of convolutional layers and added concatenation operations instead of addition and convolution operations to concatenate feature maps from different layers. Instead of an addition operation as shown in the blue dashed box of FPN (see FIGURE 3), this CFP employs a concatenation (blue dashed box in FIGURE 4 or CONCAT 1 in FIGURE 5) operation for merging 2 \times up-scaled feature channels of the deeper layer and feature channels of the shallow layer. It is noticed that there is no concatenation of features from different layers for Scale 1 of this CFP, as shown inside the red dashed line box of FIGURE 5. In addition, instead of addition as in the residual block of ResNet (Residual Network), we concatenate these features and their convoluted results (see CONCAT 2 in FIGURE 5) together. This replacement saves significant computational time since concatenation is not considered an algebraic operation. Furthermore, instead of 8 convolutional layers (black dashed box in FIGURE 3) of YOLOv3, we employ at most 4 convolutional layers. The number of convolutional layers can be adjusted to trade accuracy and efficiency. This CFP employs 2, 3, and 1 convolutional layers on Scale 1, Scale 2, and Scale 3, respectively.

B. BI-FUSION CONCATENATED FEATURE PYRAMID NETWORK

In addition to CFP, our BIF-MSP network also creates a Bi-Fusion Module (BFM) to fuse feature maps with both

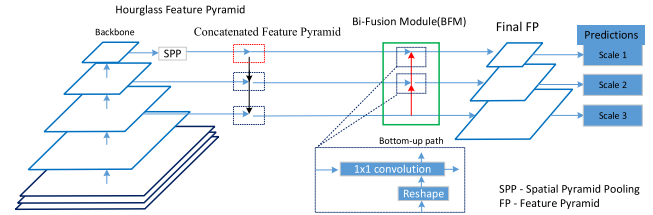


FIGURE 6. Architecture of the proposed BFM (green-dashed box).

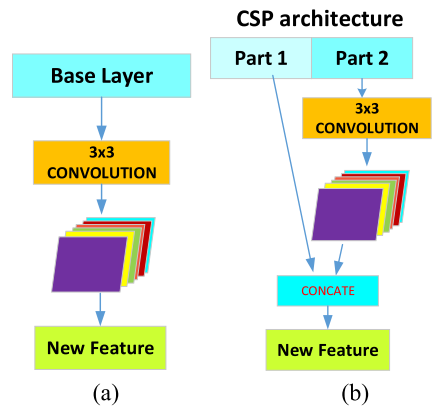


FIGURE 7. (a) Original backbone. (b) CSP architecture.

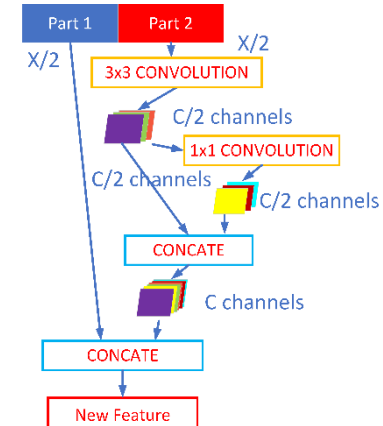


FIGURE 8. Mixed stage partial network.

the top-down and bottom-up mechanisms to generate flexible FPs for small object detection. The first direction is a *top-down path*, which is achieved by forming an hourglass FP. The second direction is a *bottom-up path* that uses BFM to generate final FP layers by concatenating reshaped features of the shallower layer of a final FP and features of a current layer of an hourglass FP. With this bifusion mechanism, an object with a small size (even if it is down-sampled to 1 pixel) can reappear at shallower layers. The green dashed box of FIGURE 6 shows the basic structure of BFM. Moreover, in case that a light backbone is adopted, the proposed BFM can further improve its efficiency for object detection in real time.

C. MIXED STAGE PARTIAL BACKBONE

For edge computing, we adopt our previous framework to further reduce computational load, *i.e.*, a lightweight Cross Stage Partial Network (CSPNet) [42]. This CSPNet has been adopted in YOLO v4. It respects the variability of the

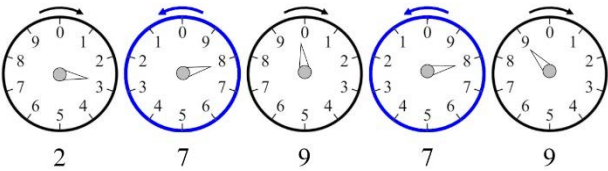


FIGURE 9. Different reading rules to interpret a dial in a dial-type meter.

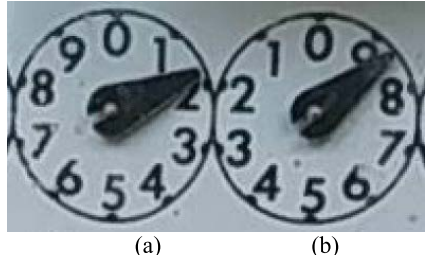


FIGURE 10. Ambiguous cases between (a) and (b).

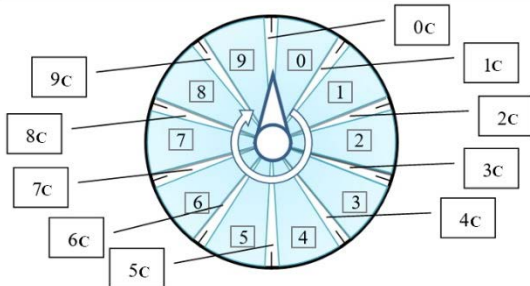


FIGURE 11. Twenty labels are used to label a dial meter.

gradients by integrating feature maps from the beginning and the end of a network stage, as shown in FIGURE 7. The CSPNet separates the feature map of the base layer into two parts, where one part will go through a dense block and a transition layer; the other part is then combined with the transmitted feature map to the next stage. Separation can not only balance the computation of each layer, but also reduce memory traffic jam. It is noticed that only one convolution layer is applied for feature extraction in this CSPNet. To further enrich the feature maps, this paper proposes a Mixed Stage Partial (MSP) network to generate more features from cheap operations. FIGURE 8 shows the architecture of MSPNet. Compared to the CSP net, only C/2 channels are generated by 3×3 convolution and further processed by 1×1 convolution, and then concatenated to generate another set of feature maps with C channels. Since only half channels, i.e., C/2 are generated, more efficiency can be gained. In addition to efficiency, greater accuracy can be gained since an additional feature extraction layer is added. Its conference version [38] is proposed for vehicle detection rather than ARM.

D. LABELING AND TRAINING

Most of current AMR systems can read 0-9 digits only from cyclometers. This paper proposes a new AMR system to read digits not only from cyclometers but also from dial-type meters. As shown in FIGURE 9, there are two reading rules to interpret a dial in a dial-type meter, *i.e.* clockwise

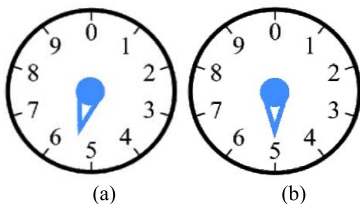


FIGURE 12. Cases for labeling a dial-type digit. (a) '5' sector. (b) '5C' sector.

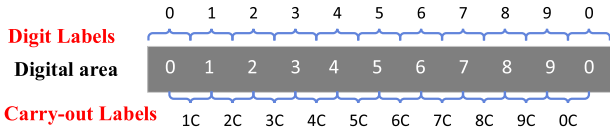


FIGURE 13. Labeling for a cyclometer.



FIGURE 14. The case of an "in-between" digit in a cyclometer.

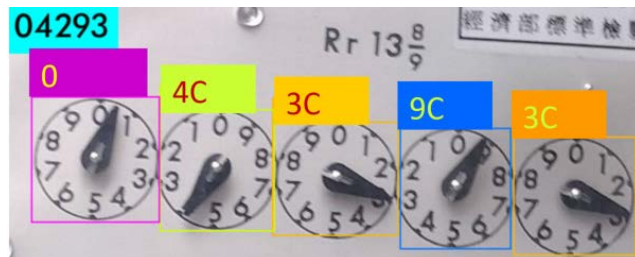
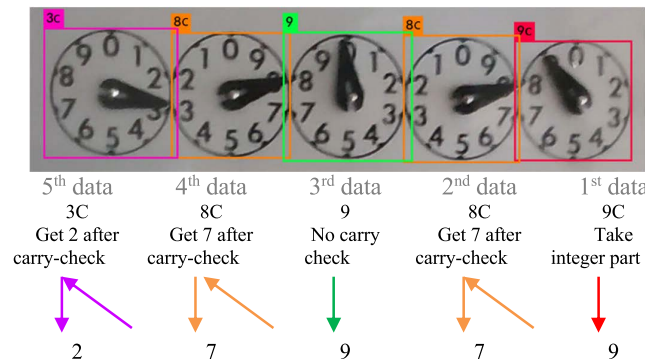
and anticlockwise. The two rules are applied interactively to interpret dials based on their positions; one is clockwise and then anticlockwise. In real cases, these two rules will confuse the trained detector and result in the failure to recognize dials with similar visual patterns. As shown in the arrows in FIGURE 10(a) and FIGURE 10(b), they have similar arrow patterns (pointing to the same direction), but should be interpreted differently. When a meter is small, the outer feature (its surrounding numbers) will become blurred and cannot provide useful information for the classifier to discriminate the two cases in FIGURE 10. To tackle this confusion problem, this paper considers that they are the same and share the same label. Thus, the cases in FIGURE 10 are labeled as the same digit '1'. They will be further identified according to their positions (odd or even).

This paper uses twenty labels to label a dial-type meter. As shown in FIGURE 11, twenty labels are used to label a dial meter and can be divided into two categories, *i.e.*, "digit" and "carry-out" categories. In FIGURE 11, for all blue intervals bounded by two digits, they belong to the category "digit" that includes digits from '0' to '9'. When an arrow points to a digit 'X', it will be in the "carry-out" category and labeled as an 'XC'. As in the example shown in FIGURE 11, all the white sectors are in the "carry-out" category and labeled as from '0C' to '9C'. FIGURE 12 shows two cases of labeling a digit '5' on a dial-type meter. In FIGURE 12 (a), the arrow is in the "digit" interval and is thus labeled '5'. FIGURE 12 (b) is labeled as '5C' since the arrow points to '5'. All the recognized results located within the carry-out interval will be further identified via a carry-out re-checking process at the post-processing stage.

As for the digits on a cyclometer, the number of labels used is also twenty. As shown in FIGURE 13, the labels are also divided into two categories, *i.e.* "digit" and "carry-out" categories. If a digit 'X' is shown, it is in the category "digit"

TABLE 1. Categories and labels are used to label a meter.

Digit Cat.	0	1	2	3	4	5	6	7	8	9
Carry Cat.	0C	1C	2C	3C	4C	5C	6C	7C	8C	9C
Meter Cat.	Dial	Digit								

**FIGURE 15.** Errors caused by a carry-out status. ‘3C’ should be ‘2’.**FIGURE 16.** Details of carry check to correct the string {‘3C’, ‘8C’, ‘9’, ‘8C’, ‘9C’} to {‘2’, ‘7’, ‘9’, ‘7’, ‘9’}.

and is labeled as ‘X’. If a digit goes from X to (X+1), it is in the “carry-out” status and is labeled as ‘XC’. For example, in FIGURE 14, the rightmost digit is labeled as ‘3C’ since it is going from 2 to 3. Table 1 lists all categories and labels used to label a meter. Three categories are used in this paper; that is, digit category, carry-out category, and meter category. The meter category includes two elements to define the ROIs of the dial meters and the cyclometers, respectively. Thus, the total number of labels is 42, i.e., $20 \times 2 + 2$.

E. CARRY-OUT RECHECKING METHOD

After detecting the counter region and digits by the BIF-MSP network, some errors still occur due to the “in-between” problem caused by digits’ carrying-out statuses. As shown in FIGURE 15, the third digit should be 2 but its indicator makes it recognized as ‘3C’ since the second digit is ‘9’. This section proposes a carry-out rechecking method to correct its value. Assume there are K digits in a meter. In the detection stage the K digits are labeled as $D_K, \dots, D_k, \dots, D_1$, where $D_k \in D_k \in \{0, 1, \dots, 9\}$. Also, let the corrected digits be represented as $N_K, \dots, N_k, \dots, N_1$. Then, the k th digit will be corrected as

$$N_k = \begin{cases} D_k, & \text{if } D_k \notin \text{CarryCategory}, \\ D_k, & \text{if } D_k \in \text{CarryCategory and } k=1, \\ D_k - 1, & \text{if } D_k \in \text{CarryCategory and } N_{k-1} > 5, \\ D_k, & \text{if } D_k \in \text{CarryCategory and } N_{k-1} \leq 5. \end{cases} \quad (1)$$

TABLE 2. Details of our dataset.

	Dial-display	Cyclometer-display	Total
Train	245	98	343
Validation	254	90	344
Test	427	104	531
total	926	292	1218

Based on Eq.(1), N_k is updated from $k = 1$ to K . As shown in FIGURE 15, the first, second, and fourth digits (from right to left) are updated to 3, 9, and 4, respectively, by dropping ‘C’, and the third digit is changed to 2 due to the third rule. Finally, the meter reads “04293”. FIGURE 16 shows the details of carry re-checking to correct the digits {‘3C’, ‘8C’, 9, ‘8C’, ‘9C’} to {2, 7, 9, 7, 9}.

IV. EXPERIMENTAL RESULTS

To evaluate the performance of our system, an in-house dataset is collected that includes 1218 images. Table 2 lists the details of the numbers of different types of meters for training, validation, and testing, respectively. All data is collected over half a year to record the variations of meters under different lighting conditions, weather conditions, and positions. This dataset can be publicly accessed by the URL: <http://140.113.110.150:5000/sharing/52HCvjly2>. In addition to this in-house dataset, two other public datasets [38], [39] have been adopted for the performance evaluation of the AMR system. The first one [38] is collected to recognize cyclometer meters and the second one [39] is for recognizing dial-type meters. For the first dataset [38], there are different conditions that affect the accuracy of the reading of meters including blurring, reflections, low contrast, broken glass, dirt, etc. It includes 2000 images that are split into three sets; that is, training (800 images), validation (400 images), and testing (800 images). For the second dataset [39], there are 2000 dial-type meters, 903 of which are for 4 dials and 1097 for 5 dials. It was divided into three subsets that included 1200 images for training, 400 images for validation, and the remaining 400 images for testing. It includes various challenges in meter recognition such as low contrast, low-end cameras, low lighting conditions, high compression ratios, skewing, etc. In addition, clockwise and counterclockwise dials also alter the accuracy of meter reading.

To evaluate performance, the accuracy of recognizing “individual” digits on meters is defined as the number of correctly recognized digits divided by the number of digits in the test set. In addition, the accuracy of meter recognition is defined as the number of correctly recognized meters divided by the number of meters in the test set; that is,

$$\text{MeterAccucy} = \frac{1}{M} \sum_{i=1}^M \text{Match}(R(i), G(i)),$$

where M is the total number of meters in the test set, $R(i)$ and $G(i)$ are the recognized string and ground truth for the i th meter, respectively. In addition, $\text{Match}(X, Y) = 1$ if $X = Y$, and 0 if $X \neq Y$.

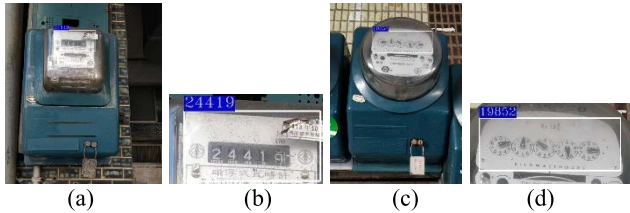


FIGURE 17. Meter reading results. (b) Result of reading a cyclometer from (a). (d) Result of reading a dial meter from (c).



FIGURE 18. Meter reading results. (b) Result of reading a dirty dial meter from (a). (d) Result of reading a dark cyclometer from (a).

FIGURE 17 shows the results of meter reading. (b) is the result of reading a cyclometer from (a). (d) is the result of reading a dial meter from (c). It is not necessary to reload the model used in our AMR system by reading a cyclometer or a dial meter. Additionally, our proposed AMR system can read meters, even though they are captured in noisy or poor lighting environments. FIGURE 18(b) shows the case of reading a dial meter in noisy conditions from FIGURE 18 (a). It is more challenging to read meters from dark environments. FIGURE 18 (d) shows the result of reading a cyclometer from (c) in a dark environment. Our AMR system can also read multiple meters from the same image. FIGURE 19 shows two cases where multiple meters were read from the same image. All digits are correctly detected and read.

To make fair comparisons, three well-known detectors are adopted in this paper, namely, Faster-CNN [20], SSD [21], and YOLO [22]. In the literature, they were adopted in most SoTA CNN-based methods [23], [24], [25], [26], [27], [28], [29], [30], [31], [32] to read different meters. In this paper, they are adopted as baselines to evaluate the performance of our BIF-MSP model. Furthermore, the RefineDet net [34] is also compared in this paper. Table 3 shows the accuracy comparisons among different methods without using any carry-out correction. In this table, the “Individual” column means the average accuracy of each digit to be correctly recognized and the “Meter” column means the average accuracy of all digits on a meter that should be correctly recognized. Faster-RCNN performs the worst in terms of accuracy and efficiency. YoloV3 performs better than SSD in both the “Individual” and “Meter” categories, even though the input size is smaller. The accuracy of RefineDet Net is better than that of YOLO v3 but with lower *fps*. The accuracy of our method performs the best among all the compared methods in both the categories “Individual” and “Meter”. YOLO v4 performs better than YOLO v3, SSD, RefineDet, and FasterRCNN. It also performs better than our method with the backbone “Darknet-53”. However, when the CSP-Net backbone was adopted, the efficiency of our method is better than that of YOLO v4, but with comparable accuracy. Our method with the MSP-Net backbone performs the best among all the methods (including YOLO V4). Interestingly, most

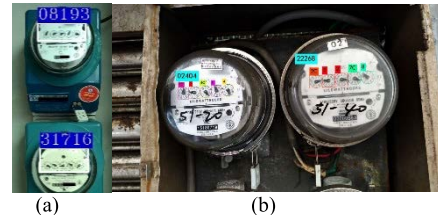


FIGURE 19. Results of reading multiple meters. (a) Cyclometers. (b) Dial meters.



FIGURE 20. Failure case of meter reading due to the problem of “carry-out”. The correct result is “7511”.

TABLE 3. Accuracy comparisons among different methods without using a carry-out correction.

Methods	backbone	size	Dial-display		Cyclometer-display		<i>fps</i>
			Individual	Meter	Individual	Meter	
FasterRCNN	VGG-16	416×416	81.78%	35.83%	89.42%	34.43%	1.98
SSD [21]	VGG-16	300×300	83.70%	36.19%	89.75%	35.94%	39.56
SSD [21]	ResNet101	321×321	85.82%	37.38%	92.58%	37.12%	44.01
SSD-512 [21]	VGGNet-16	512×512	86.65%	38.12%	93.37%	38.46%	19.43
RefineDet-512 [34]	VGG-16	512×512	87.53%	39.35%	94.19%	39.87%	34.83
YOLOv3 [22]	Darknet-53	416×416	86.91%	38.62%	93.42%	39.68%	45.74
YOLOv4 [37]	CSP-Net	416×416	90.83%	44.21%	96.72%	42.01%	48.26
Our method	Darknet-53	416×416	88.78%	41.84%	95.42%	40.63%	45.97
Our method	CSP-Net	416×416	90.25%	43.42%	96.49%	41.76%	48.76
Our method	MSP-Net	416×416	91.67%	45.58%	97.58%	42.95%	49.86

TABLE 4. Accuracy comparisons among different methods with using a carry-out correction.

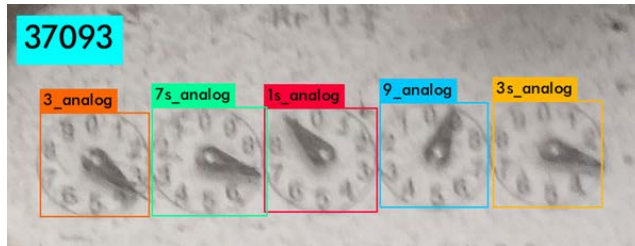
Methods	backbone	size	Dial (meter)	Cyclometer (meter)	fps
FasterRCNN[20]	VGG-16	416×416	89.93%	83.65%	1.77
SSD[21]	VGG-16	300×300	91.14%	78.08%	39.15
SSD[21]	ResNet101	321×321	91.76%	79.96%	43.67
SSD-512[21]	VGG-16	512×512	92.06%	80.45%	19.02
RefineDet-512[34]	VGG-16	512×512	92.93%	82.39%	34.63
YOLOv3 [22]	Darknet-53	416×416	92.27%	81.64%	46.29
YOLOv4 [37]	CSP-Net	416×416	97.39%	88.45%	48.31
Our method	Darknet-53	416×416	95.78%	85.58%	46.65
Our method	CSP-Net	416×416	97.15%	87.63%	48.82
Our method	MSP-Net	416×416	98.31%	89.13%	49.02

methods perform better in cyclometers than dial meters due to the ambiguous cases shown in FIGURE 10. However, in the “Meter” category, the accuracies of all methods in the cyclometer meters are lower than those of the dial-type meters due to the “carry-out” problem. As shown in FIGURE 20, the recognized result is “7512” but should be “7511”. The fourth pattern in FIGURE 20 was incorrectly recognized as ‘2’ since it would soon be ‘2’. It should be recognized as ‘1’ but with visual features similar to ‘2’. The same problem also occurs in dial-type meters whose main features depend on their arrows. On the other hand, for the digits in a cyclometer, the features used are shapes. The in-between problem causes more distortions in the shape of a digit than in the direction of an arrow. Therefore, more errors will occur on the cyclometers than on the dials, thus resulting in lower accuracy in the “meter” category for all methods.

TABLE 4 tabulates the accuracy comparisons among different methods if our proposed carry-out rechecking method was adopted. Here, only the results of the “meter” category are listed in Table 4. Compared to TABLE 3, the accuracy

TABLE 5. Accuracy comparisons among different methods with using carry-out correction and mirroring.

Methods	Outer feature			Inner feature with position		
	Dial	Cyclometer	fps	Dial	Cyclometer	fps
FasterRCNN	86.31%	79.17%	1.85	89.93%	83.65%	1.77
SSD[21]	88.18%	74.76%	39.37	91.14%	78.08%	39.15
SSD[21]	89.03%	75.52%	43.82	91.76%	79.96%	43.67
SSD-512[21]	89.62%	76.68%	19.38	92.06%	80.45%	19.02
RefineDet-512[34]	90.05%	79.08%	34.91	92.93%	82.39%	34.63
YOLOv3 [22]	89.89%	77.95%	45.53	92.27%	81.64%	45.31
YOLOv4 [37]	91.35%	80.12%	45.31	95.69%	86.53%	47.65
Our method	92.85%	81.85%	45.94	97.31%	88.13%	48.56

**FIGURE 21.** Failure case of meter reading due to the ambiguous problem of digit labeling. The expected result should be “37893”.

improvements are significant (almost double) if the rechecking method is adopted. As described above, the in-between problem creates more distortions in the shape of a digit than in the direction of an arrow. Thus, for all methods, the accuracies in digit-type meters are lower than those in dial-type meters. From this table, our method still performs the best among all methods (including YOLO v4).

As shown in FIGURE 10(a), there are two rules for interpreting a dial in a dial-type meter; that is, clockwise and anticlockwise. The two rules will confuse the learner and thus degrade its accuracy. For a dial in a dial-type meter, it can be identified according to its “inner” feature, that is, the orientation of the arrow or its “outer” feature, that is, the printed numbers. When the meter is large, the cases in FIGURE 10(a) and FIGURE 10(b) can be easily identified, since their outer features are clear enough. However, in case the meter is small or blurred, the inner feature “arrow orientation” will dominate the final decision and result in the failure to identify the two cases (as shown in FIGURE 21). Then, FIGURE 10(b) will be misclassified as ‘1’. Thus, it is better to let the two cases share the same label and be further discriminated according to their positions (odd or even). TABLE 5 tabulates the comparisons between the “outer” feature and the “inner” one with position. FIGURE 21 shows the failure case of meter reading due to this ambiguous problem. The third digit should be detected as ‘9’ and then corrected as ‘8’. However, it was incorrectly detected as ‘1’ and then corrected as ‘0’ due to its ambiguous and unclear “outer” feature. Therefore, in Table 5, clearly, the “outer” feature performs worse than the “inner” feature. Both the efficiencies of the “inner” feature and the “outer” feature are similar. Compared to other methods, our method still performs the best when only the “outer” feature is adopted.

TABLE 6 tabulates the comparisons among different light backbones. The lightweight backbones adopted here for

TABLE 6. Accuracy comparisons with a lightweight backbone and carry-out correction on Jetson TX2.

Methods	backbone	size	Dial	Cyclometer	fps
SSD[21]	MobileNet[35]	416×416	83.54%	78.53%	27.65
YOLO Tiny [22]	Tiny-15	416×416	78.92%	72.12%	33.27
Our method	PeLee [33]	416×416	92.38%	81.73%	28.35
Our method	CSP-Net [42]	416×416	94.03%	83.85%	31.28
Our method	MSP-Net	416×416	95.16%	85.05%	31.86

TABLE 7. Average accuracies of our method if the rightmost digit is not included.

Methods	backbone	size	Dial	Cyclometer
Our method	PeLee [36]	416×416	95.73%	89.84%
Our method	CSP-Net [42]	416×416	97.13%	92.58%
Our method	MSP-Net	416×416	98.54%	93.69%

TABLE 8. Accuracy comparisons among different methods based on the public dataset of cyclometers [38].

Methods	backbone	size	Individual	No Carry-out-correction		Carry-out-Correction	
				Meter	FPS	Meter	FPS
SSD [21],[29]	VGG-16	300x300	93.37	91.38	56.72	92.62	56.13
SSD [21],[29]	ResNet101	321x321	93.17	91.06	45.77	92.37	45.11
SSD-512 [21], [29]	VGG-16	512x512	95.07	92.87	34.52	94.12	33.96
RefineDet [34]	VGG-16	512x512	92.55	90.05	18.04	91.11	17.61
FCN [27]*	VGG-16	224x224	-	93.87	46.61	-	-
Multitask [23]*	VGG-19	416x416	95.96	89.12	46.6	-	-
CRNet [23]*	Darknet-19	416x416	98.30	94.25	32.9	-	-
CDCC-Net [24]	CSP-Net	416x416	-	94.75	44.20	-	-
YOLOv3 [26]	Darknet-19	416x416	94.37	91.87	45.35	93.37	44.82
YOLO v4 [42]	CSP-Net	416x416	98.39	96.32	46.61	97.48	45.54
Our method	Darknet-53	416x416	96.45	95.06	45.54	96.76	44.61
Our method	CSP-Net	416x416	97.68	95.81	46.89	97.27	45.68
Our method	MSP-Net	416x416	99.42	97.26	47.54	98.87	46.75

* All the data are cited from [24] and the FPS values are recalculated based on YOLO V4.

comparisons are MobileNet [35], YOLO Tiny [22], PeLee [36], our CSP [42], and our BIF-MSP. Our CSP backbone had been adopted in YOLO V4 [37]. The platform for this performance evaluation is based on Jetson TX2. The best *fps* was obtained from YOLO Tiny but with the lowest accuracy. The worst efficiency was obtained from SSD with Mobile Net. Our method with the BIF-MSP backbone performs the best in terms of both accuracy and efficiency. Actually, the rightmost digit in a meter moves much faster than other digits and changes per second. Therefore, it often stays in the carry-out state and leads to errors in meter reading. However, due to its fast changes, it plays an unimportant role in billing. TABLE 7 lists the average accuracies of our method if the rightmost digit is not included. If this rightmost digit is ignored, the final accuracy of the “dial -type” meter is up to 98.14%. All of the above experiments have proved the superiority of our method for both dial-type and digit-type meters.

TABLE 8 lists the accuracy comparisons between different methods for reading cyclometers based on the open dataset [38]. Since the minimum size of a digit is 35 × 63, the accuracies for all compared methods are much higher. In this paper, seven SoTA methods [21], [23], [24], [26], [27], [31], [42] were compared. Among them, the four methods [23], [24], [26], [27] were specially designed to read cyclometers. Regarding the failure cases, errors occur mainly due to the in-between problem, i.e., digits to be carried out. The input size of FCN [27] is the smallest, and thus its accuracy is lower. As described before, YoloV3 [26] performs better than SSD even in this open dataset [38]. As for CDC-Net [24], to speed up the efficiency of its previous framework [23], a light

TABLE 9. Accuracy comparisons among different methods based on the public dataset of dial meters [39].

Methods	Backbone	size	Individual	No Carry-correction		Carry-Correction	
				Meter	FPS	Meter	FPS
SSD	VGG-16	300x300	88.54	42.5	56.44	74.5	56.02
SSD	ResNet101	321x321	87.95	39.5	44.71	71.5	44.25
SSD-512	VGG-16	512x512	93.79	48.5	33.6	80.5	33.19
RefineDet	VGG-16	512x512	25.97	-	-	-	-
YOLO V2	darknet19	416x416	90.14	66.5	79.43	86.5	79.05
YOLO V3Tiny [22]	Tiny-15	416x416	82.14	45.5	269.62	77.5	265.18
YOLOv3	Darknet-53	416x416	91.69	71.5	44.84	85.5	44.32
YOLOv4	CSP-Net	416x416	94.68	79.21	46.49	90.12	45.86
Our method	Darknet-53	416x416	93.22	77.75	45.13	88.54	44.96
Our method	CSP-Net	416x416	94.37	78.83	46.68	89.84	46.21
Our method	MSP-Net	416x416	95.79	80.86	47.35	91.65	46.93

backbone (modified from YOLO v4) is adopted and thus cannot extract enough semantic features to read the meters. Although its efficiency has been significantly improved, the improvement in accuracy is minor. However, our method is still the best. This paper proposes a carry-out rechecking method to further improve the accuracy of meter recognition. In TABLE 8, the seventh column lists the improved accuracies of meter recognition after performing this rechecking task. The rightmost column shows the FPSs of meter recognition after carry-out rechecking for all methods. The task of rechecking slightly reduces their FPSs.

TABLE 9 shows the accuracy comparisons among different methods to recognize dial-type meters in the public dataset [39]. Compared to cyclometers (see Table 8), the existence of clockwise and counterclockwise interpretation rules makes the average accuracy of reading dial meters lower. Since the accuracy of RefineDet to recognize individual dials is too low, its other performance evaluations are not performed here. The YOLO V3Tiny got the fastest FPS but with lower accuracy. The fifth column of TABLE 9 shows the accuracy comparisons of meter recognition without using our carry-out rechecking technique. The effect of the in-between problem will significantly degrade the accuracy of reading a whole meter. Table 9 shows the accuracy comparisons of meter recognition without/with the carry-out rechecking technique. Even with the carry-out rechecking method, the FPSs for all methods do not change significantly. However, the accuracy improvements are significant. For example, for our method, the improvement is about 10.79% from 80.86% to 91.65%. All of the above experimental results demonstrate the superiority of our method in terms of accuracy and efficiency.

V. CONCLUSION AND FUTURE WORK

This paper has proposed an AMR system based on a lightweight CNN architecture that reads both dial-type and cyclometers in real time. Most errors in meter reading are caused by the in-between problem of digits. To deal with this problem, a carry-out rechecking method has been proposed to determine the real value of each digit in a meter. Due to the lightweight architecture, the proposed AMR system can achieve 30 fps on the NVidia TX2 platform. Our AMR system can read dial-type meters even if their dials are designed with an anticlockwise or clockwise rule. Extensive experiments show that the proposed method achieves SoTA results under

different datasets in terms of accuracy and efficiency in reading the meters. After analysis, most errors occur in the rightmost digits due to its quick changes. Accuracy can be further improved if multiple frames are used to vote confidences on each recognized digit. Additionally, if historical records of each analyzed meter are provided, better accuracies can be obtained by setting constraints on the current meter reading; that is, the value of the current meter reading record should be larger than its previous record.

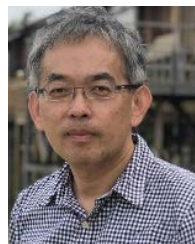
REFERENCES

- [1] (Sep. 30, 2022). *Automatic Meter Reading*. [Online]. Available: https://en.wikipedia.org/wiki/Automatic_meter_reading
- [2] T. Khalifa, K. Naik, and A. Nayak, “A survey of communication protocols for automatic meter reading applications,” *IEEE Commun. Surveys Tuts.*, vol. 13, no. 2, pp. 168–182, 2nd Quart., 2011.
- [3] R. Hammons and J. Myers, “Smart city,” *IEEE Internet Things Mag.*, vol. 7, pp. 1–2, 2019.
- [4] U. E. I. Administration. (2019). *Electric Power Annual 2018*. [Online]. Available: <https://www.eia.gov/electricity/annual/pdf/epa.pdf>
- [5] G. Salomon, R. Laroca, and D. Menotti, “Deep learning for image-based automatic dial meter reading: Dataset and baselines,” in *Proc. Int. Joint Conf. Neural Netw. (IJCNN)*, Jul. 2020, pp. 1–8.
- [6] A. Alsharif, M. Nabil, S. Tonyali, H. Mohammed, M. Mahmoud, and K. Akkaya, “EPIC: Efficient privacy-preserving scheme with EtoE data integrity and authenticity for AMI networks,” *IEEE Internet Things J.*, vol. 6, no. 2, pp. 3309–3321, Apr. 2019.
- [7] B. Bera, S. Saha, A. K. Das, and A. V. Vasilakos, “Designing blockchain-based access control protocol in IoT-enabled smart-grid system,” *IEEE Internet Things J.*, vol. 8, no. 7, pp. 5744–5761, Apr. 2021.
- [8] M. Rodriguez, G. Berdugo, D. Jabba, M. Calle, and M. Jimeno, “HD-MR: A new algorithm for number recognition in electrical meters,” *Turkish J. Electr. Eng. Comput. Sci.*, vol. 22, no. 1, pp. 87–96, 2014.
- [9] Y. Tang, C. W. Ten, C. Wang, and G. Parker, “Extraction of energy information from analog meters using image processing,” *IEEE Trans. Smart Grid*, vol. 6, no. 4, pp. 2032–2040, Jul. 2015.
- [10] I. Gallo, A. Zamberletti, and L. Noce, “Robust angle invariant GAS meter reading,” in *Proc. Int. Conf. Digit. Image Comput., Techn. Appl. (DICTA)*, Nov. 2015, pp. 1–7.
- [11] J. Matas, O. Chum, M. Urban, and T. Pajdla, “Robust wide baseline stereo from maximally stable extremal regions,” in *Proc. Brit. Mach. Vis. Conf.*, vol. 1, 2002, pp. 384–393.
- [12] C. Li, Y. Su, R. Yuan, D. Chu, and J. Zhu, “Light-weight spliced convolution network-based automatic water meter reading in smart city,” *IEEE Access*, vol. 7, pp. 174359–174367, 2019.
- [13] L. Gomez, M. Rusinol, and D. Karatzas, “Cutting Sayre’s knot: Reading scene text without segmentation. Application to utility meters,” in *Proc. 13th IAPR Int. Workshop Document Anal. Syst. (DAS)*, Apr. 2018, pp. 97–102.
- [14] D. Shu, S. Ma, and C. Jing, “Study of the automatic reading of Watt meter based on image processing technology,” in *Proc. 2nd IEEE Conf. Ind. Electron. Appl.*, May 2007, pp. 2214–2217.
- [15] D. M. Oliveira, R. D. S. Cruz, and K. Bensebaa, “Automatic numeric characters recognition of kilowatt-hour meter,” in *Proc. 5th Int. Conf. Signal Image Technol. Internet Based Syst.*, Nov. 2009, pp. 107–111.
- [16] Z. Cai, C. Wei, and Y. Yuan, “An efficient method for electric meter readings automatic location and recognition,” *Proc. Eng.*, vol. 23, pp. 565–571, Mar. 2011.
- [17] Y. Zhang, S. Yang, X. Su, E. Shi, and H. Zhang, “Automatic reading of domestic electric meter: An intelligent device based on image processing and ZigBee/Ethernet communication,” *J. Real-Time Image Process.*, vol. 12, no. 1, pp. 133–143, Jun. 2013.
- [18] L. A. Elrefaei, A. Bajaber, S. Natheir, N. AbuSanab, and M. Bazi, “Automatic electricity meter reading based on image processing,” in *Proc. IEEE Jordan Conf. Appl. Electr. Eng. Comput. Technol. (AEECT)*, Nov. 2015, pp. 1–5.
- [19] A. Anis, M. Khaliluzzaman, M. Yakub, N. Chakraborty, and K. Deb, “Digital electric meter reading recognition based on horizontal and vertical binary pattern,” in *Proc. 3rd Int. Conf. Elect. Inf. Commun. Technol. (EICT)*, Khulna, Bangladesh, Dec. 2017, pp. 1–6.

- [20] S. Ren, K. He, R. Girshick, and J. Sun, "Faster R-CNN: Towards real-time object detection with region proposal networks," in *Proc. Adv. Neural Inf. Process. Syst.*, 2015, pp. 91–99.
- [21] W. Liu, D. Anguelov, D. Erhan, C. Szegedy, S. Reed, C. Y. Fu, and A. C. Berg, "SSD: Single shot MultiBox detector," in *Proc. ECCV*, Oct. 2016, pp. 21–37.
- [22] J. Redmon and A. Farhadi, "YOLOv3: An incremental improvement," 2018, *arXiv:1804.02767*.
- [23] R. Laroca, V. Barroso, M. A. Diniz, G. R. Gonçalves, W. R. Schwartz, and D. Menotti, "Convolutional neural network for automatic meter reading," *J. Electron. Imag.*, vol. 28, no. 1, Feb. 2019, Art. no. 013023.
- [24] R. Laroca, A. B. Araujo, L. A. Zanlorensi, E. C. De Almeida, and D. Menotti, "Towards image-based automatic meter reading in unconstrained scenarios: A robust and efficient approach," *IEEE Access*, vol. 9, pp. 67569–67584, 2021.
- [25] K. He, X. Zhang, S. Ren, and J. Sun, "Deep residual learning for image recognition," in *Proc. IEEE Conf. Comput. Vis. Pattern Recognit. (CVPR)*, Jun. 2016, pp. 770–778.
- [26] S. Liao, P. Zhou, L. Wang, and S. Su, "Reading digital numbers of water meter with deep learning based object detector," in *Proc. Chin. Conf. Pattern Recognit. Comput. Vis.*, 2019, pp. 38–49.
- [27] A. Calefati, I. Gallo, and S. Nawaz, "Reading meter numbers in the wild," in *Proc. Digital Image Comput., Techn. Appl. (DICTA)*, Dec. 2019, pp. 1–6.
- [28] C. Son, S. Park, J. Lee, and J. Paik, "Deep learning-based number detection and recognition for gas meter reading," *IEIE Trans. Smart Process. Comput.*, vol. 8, no. 5, pp. 367–372, Oct. 2019.
- [29] C.-M. Tsai, T. D. Shou, S.-C. Chen, and J.-W. Hsieh, "Use SSD to detect the digital region in electricity meter," in *Proc. Int. Conf. Mach. Learn. Cybern. (ICMLC)*, Jul. 2019, pp. 1–7.
- [30] M. Waqar, M. A. Waris, E. Rashid, N. Nida, S. Nawaz, and M. H. Yousaf, "Meter digit recognition via faster R-CNN," in *Proc. Int. Conf. Robot. Autom. Ind. (ICRAI)*, Oct. 2019, pp. 1–5.
- [31] Y. Gao, C. Zhao, J. Wang, and H. Lu, "Automatic watermeter digit recognition on mobile devices," in *Proc. Int. Conf. Internet Multimedia Comput. Service*. Singapore: Springer, Aug. 2017, pp. 87–95.
- [32] F. Yang, L. Jin, S. Lai, X. Gao, and Z. Li, "Fully convolutional sequence recognition network for water meter number reading," *IEEE Access*, vol. 7, pp. 11679–11687, 2019.
- [33] L. Li, Y. Li, K. Lian, X. Bian, K. Yang, and Y. Tian, "PGC-Net: A light weight convolutional sequence network for digital pressure gauge calibration," *IEEE Access*, vol. 7, pp. 123280–123288, 2019.
- [34] T.-Y. Lin, P. Goyal, R. Girshick, K. He, and P. Dollár, "Focal loss for dense object detection," in *Proc. IEEE Int. Conf. Comput. Vis. (ICCV)*, Oct. 2017, pp. 2980–2988.
- [35] A. G. Howard, M. Zhu, B. Chen, D. Kalenichenko, W. Wang, T. Weyand, M. Andreetto, and H. Adam, "MobileNets: Efficient convolutional neural networks for mobile vision applications," in *Proc. ECCV*, 2018, pp. 1–9.
- [36] R. J. Wang, X. Li, and C. X. Ling, "Pelee: A real-time object detection system on mobile devices," in *Proc. NIPS*, 2018, pp. 1–10.
- [37] A. Bochkovskiy, C.-Y. Wang, and H.-Y. Mark Liao, "YOLOv4: Optimal speed and accuracy of object detection," 2020, *arXiv:2004.10934*.
- [38] (2019). *UFPR-AMR Dataset*. [Online]. Available: <https://web.inf.ufpr.br/vri/databases/ufpr-amr/>
- [39] (2019). *UFPR-ADMv1 Dataset*. [Online]. Available: <https://web.inf.ufpr.br/vri/databases/ufpr-admr/>
- [40] S. W. Kim, H. K. Kook, J. Y. Sun, M. C. Kang, and S. J. Ko, "Parallel feature pyramid network for object detection," in *Proc. ECCV*, 2018, pp. 234–250.
- [41] B. Bosquet, M. Muñientes, and V. M. Brea, "STDNet: A ConvNet for small target detection," in *Proc. BMVC Sep.* 2018, p. 253.
- [42] C.-Y. Wang, H.-Y. M. Liao, Y.-H. Wu, P.-Y. Chen, J.-W. Hsieh, and I.-H. Yeh, "CSPNet: A new backbone that can enhance learning capability of CNN," in *Proc. IEEE/CVF Conf. Comput. Vis. Pattern Recognit. Workshops (CVPRW)*, Jun. 2020, pp. 390–391.
- [43] C. Ping-Yang, J.-W. Hsieh, M. Gochoo, and Y.-S. Chen, "Light-weight mixed stage partial network for surveillance object detection with background data augmentation," in *Proc. IEEE Int. Conf. Image Process. (ICIP)*, Sep. 2021, pp. 3333–3337.



JIA-YUAN LIAO received the M.S. degree in computer science engineering from National Taiwan Ocean University, Keelung, Taiwan, in 2018. His research interests include low-power computer vision, image processing, pattern recognition, and deep learning.



JUN-WEI HSIEH (Member, IEEE) was an Associate Professor at the Department of Electrical Engineering, Yuan-Ze University, and a Visiting Researcher at the MIT AI Laboratory. From August 2009 to August 2019, he was a Professor and the Dean of the Department of Computer Engineering, National Taiwan Ocean University. Since August 2019, he has been a Professor with the College of AI, National Yang-Ming Chiao-Tung University. He hosted or co-hosted a lot of large-scale

AI projects from different companies and governments in the past. He has a lot of successful experiences in industrial-academic cooperation and technology transfer, especially in ITS. His research interests include AI, deep learning, smart farming, video surveillance, intelligent transportation systems, image and video processing, object recognition, machine learning, 3D printing, medical image analysis, and computer vision. In May 2019, he received the First Prize of the Ministry of Science and Technology Best Display Award and the Third Place of the AI Investment Potential Award. Due to his contributions to traffic flow estimation, he helped Elan company to receive the Gold Award from the Taipei International Computer Show, in 2019. He also received the Outstanding Research Awards of National Taiwan Ocean University, in 2012, 2016, 2017, and 2019, and the Outstanding Research Awards of Yuan Ze University, in 2006, 2007, and 2008. He and his students received the Silver Medal of 2019 National College Software Creation Competition, the Silver Medal of 2018 National Microcomputer Competition, the Best Paper Awards of Information Technology and Applications in Outlying Islands Conference, in 2013, 2014, 2016, 2017, 2018, and 2021, the Best Paper Award of Tanet 2017, the Best Paper Awards of NCWIA 2020 and 2021, and the Best Paper Awards of IS3C 2020. He also received the Best Paper Award of CVGIP Conference, in 1999, 2003, 2005, 2007, 2014, 2017, and 2018, the Best Paper Award of DMS Conference, in 2011, the Best Paper Award of IIHMSP 2010, and the Best Patent Award of Institute of Industrial Technology Research, in 2009 and 2010, respectively. He is the Program Chair of Conference on Multimedia Modeling 2011 and the Program Chair of the IEEE Advanced Video and Signal-based Surveillance (AVSS) 2019.



CHING-WEN MA received the M.S. degree from the Department of Control Engineering and the P.H. degree from the Department of Electrical and Control Engineering from National Chiao-Tung University, Hsinchu, Taiwan, in 1992 and 1998, respectively. He was a Technical Manager at Medi-aTek Inc., Hsinchu. Currently, he is an Associate Professor with the College of AI, National Yang-Ming Chiao-Tung University. His research interests include low-power computer vision, defect detection and classification, local voice control and voice assistant, sparse neural networks on FPGA, and deep learning.